Prediction of the Flow Around a Golf Ball using Different Turbulence Models

Clinton E. Smith*, Kyle D. Squires†
MAE Department, Arizona State University, Tempe, AZ
James R. Forsythe‡
Cobalt Solutions LLC, 4636 New Carlisle Pike, Springfield, OH

Several turbulence models, including Reynolds-Averaged Navier-Stokes (RANS[1]), Detached Eddy Simulation (DES[2]), and Delayed Detached Eddy Simulation (DDES[3]) are applied to prediction of sub-critical flow around a golf ball. Both non-rotating and rotating cases are considered. One of the primary goals of the work is to accurately assess the capability of the turbulence treatments to predict the flight performance of the ball and to resolve the turbulent flow structures which contribute to the delayed separation of airflow around the ball. In this abstract, predictions are presented from computations performed at a Reynolds number based on the diameter of the ball and a freestream velocity of 5.79×10^1. The flow visualizations show the baseline case of a non-rotating ball as well as a rotating ball. The time history of the lift and drag forces between the two cases are similar, but the values of the rotating case are nominally higher for all turbulence models used. Predictions of the lift and drag coefficients using RANS and DDES are in good agreement with the experimental measurements of Bearman and Harvey[4] and Choi *et al.*[5] Current investigations are focusing on the influence of the number of dimples, the dimple pattern, and the Reynolds number in the range of available experiments. This ongoing work will be presented in the full paper.

Introduction

SIMULATION of turbulent flows in engineering applications produces mean properties of the given flow, i.e., average pressure, skin friction, velocity, etc. The distinctions between the different simulation strategies used in this study are due mainly to the method in which the mean properties of the flow are computed.[6]

Reynolds-Averaged Navier-Stokes (RANS) approaches have been widely used as solutions to engineering problems involving turbulence. However, the turbulence model employed by RANS solutions averages the equations and parameterizes the turbulent motions. The fidelity of RANS models has been verified in regions exhibiting little or no flow reversal and/or separation, but it is clear that RANS models cannot accurately predict the turbulent motion in regions of massively separated flow,[7] as in the case of the golf ball.

Detached-Eddy Simulation is among the more widely applied hybrid RANS-LES techniques for prediction of massively separated flows at high Reynolds numbers. In natural applications of the technique the entire boundary layer is predicted using a RANS model, with an LES treatment of separated regions. Thus, the "RANS Region" constitutes the attached boundary layers of a flow while the "LES Region" comprises the separated regions. The interface between the RANS and LES regions is a "grey area" which has received attention since it can in some instances adversely effect the accuracy of DES predictions. These adverse effects typically arise when wall-parallel grid spacings become smaller than the boundary layer thickness and the grey area resides within the boundary layer. This lowers the eddy viscosity and, consequently, the modeled Reynolds stress. If resolved Reynolds stress developed from velocity fluctuations has not yet developed, then the total Reynolds stresses are too low and skin friction levels will be reduced.

Recently, Spalart *et al.*[3] proposed a new version of the technique, referred to as Delayed Detached-Eddy Simulation (DDES), that addresses this shortcoming of the baseline version of the method, which will be referred to as DES97[2] throughout. The new version addresses natural applications where it is desired to maintain RANS behavior throughout the boundary layer. As described in their work,[3] DDES is based on a simple modification to DES97 and is similar to the proposal of Menter and Kuntz[8] developed for the SST model. Assessment of DDES reported by Spalart *et al.*[3] was favorable and motivated the current application to the flow over a golf ball.

*Research Assistant
†Professor, AIAA Member
‡Director of Research, Senior Member AIAA

Adverse effects impacting DES97 arise when the mesh has very fine wall-parallel grid spacings and/or thick boundary layers. Both of these attributes are characteristic of the flow over the golf ball on typical grids and thus the present effort considering the subcritical flow over the golf ball is anticipated to expose flaws in DES97, . In particular, while the prediction of the turbulent boundary layers on the golf ball by the two models are anticipated to be different, differences in the LES region are also possible. An adverse effect on the LES region in DDES could, for example, degrade predictions of the unsteady features of the wake and in turn influence the back pressures and drag coefficient.

Presented in the following sections is an overview of the simulation approach followed by a representative sampling of results, and finally summary of the work performed to date. As described below, the current computations are presented of the flow at $Re = 1.58 \times 10^2$, which can be compared to results obtained by.... Calculations for different Reynolds numbers and other parameter combinations will be presented in the full paper.

Detached-Eddy Simulation

Spalart-Allmaras Model

The baseline version DES97 is formulated using the Spalart-Allmaras (referred to as 'S-A' throughout) one-equation model,[1] which solves solves a single partial differential equation for a variable $\widetilde{\nu}$ which is related to the turbulent viscosity. The model includes a wall destruction term that reduces the turbulent viscosity in the log layer and laminar sublayer and trip terms that provides a smooth transition from laminar to turbulent flow.

Detached-Eddy Simulation

The baseline formulation, DES97, is based on a modification to the Spalart-Allmaras RANS modelsuch that the model reduces to its RANS formulation near solid surfaces and to a subgrid model away from the wall. The basis is to attempt to take advantage of the usually adequate performance of RANS models in the thin shear layers where these models are calibrated and LES for resolution of geometry-dependent and three-dimensional eddies. The DES formulation is obtained by replacing in the S-A model the distance to the nearest wall, d, by $\widetilde{d}$, where $\widetilde{d}$ in DES97 is defined as,

$$\widetilde{d} \equiv \min(d, C_{DES}\Delta), \tag{1}$$

where the lengthscale Δ is the largest distance between the cell center under consideration and the cell center of the neighbors (i.e., those cells sharing a face with the cell in question). In "natural" applications of DES, the wall-parallel grid spacings (e.g., streamwise and spanwise) are typically on the order of the boundary layer thickness and the S-A RANS model is retained throughout the boundary layer, i.e., $\widetilde{d} = d$. Consequently, prediction of boundary layer separation is determined in the "RANS mode" of DES. Away from solid boundaries, the closure is a one-equation model for the SGS eddy viscosity. The constant $C_{DES} = 0.65$ was set in homogeneous turbulence[9] and is used without modification in this study.

The new version of the model, DDES, modifies the formula (1) in order to preserve RANS treatment of the boundary layer. Essentially, the spirit of the modification (1) is to utilize information concerning the lengthscale of the turbulence as predicted by the model, in addition to the wall distance and local grid spacing. As reported by Spalart *et al.*,[3] the modification is analogous to that developed by Menter and Kuntz which uses the blending function F_2 of the SST model to shield the boundary layer and "delay LES function.[8]" The argument of this function is $\sqrt{k}/(\omega \mathrm{y})$, which is the ratio between the internal length scale $\sqrt{k}/\omega$ of the k-ω turbulence model and the distance to the wall (y or d). The F function equals 1 in the boundary layer and falls to 0 rapidly at the edge of the boundary layer. The S-A model does not use an internal length scale such as $\sqrt{k}$ / ω but instead involves the parameter r, which is also the squared ratio of a model length scale to the wall distance (the length scale is not internal in that it involves the mean shear rate). For DDES, the parameter r is slightly modified relative to the S-A definition, in order to apply to any eddy-viscosity model, and be slightly more robust in irrotational regions:

$$r_d \equiv \frac{\nu_t + \nu}{\sqrt{U_{i,j}U_{i,j}}\kappa^2 d^2}, \tag{2}$$

where ν_t is the kinematic eddy viscosity, ν the molecular viscosity, $U_{i,j}$ the velocity gradients, κ the Karman constant, and d the distance to the wall. Similar to r in the S-A model, this parameter equals 1 in a logarithmic layer, and falls to 0 gradually towards the edge of the boundary layer. The addition of ν in the numerator corrects the very near-wall behavior by ensuring that r_d remains away from 0. In the S-A model, $\widetilde{\nu}$ can be used instead of $\nu_t + \nu$. The subscript "d" represents "delayed."

The quantity r_d is used in the function:

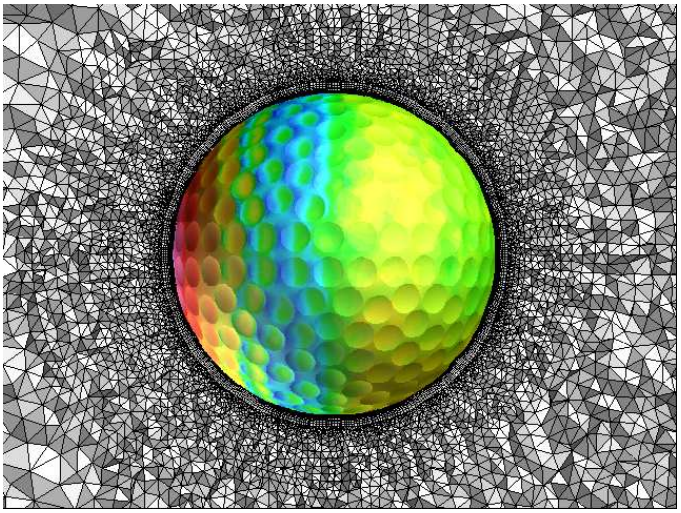

Fig. 1 Cross-section of the grid in the vicinity of the golf ball.

$$f_d \equiv 1 - tanh([8r_d]^3), \tag{3}$$

which is designed to be 1 in the LES region, where $r_d << 1$, and 0 elsewhere (and to be insensitive to r_d exceeding 1 very near the wall). It is similar to 1 - F_2, and rather steep near $r_d = 0.1$.

The values 8 and 3 for the constants in (3) are based on intuitive shape requirements for f_d, and on tests of DDES in the flat-plate boundary layer. These values for the coefficients ensure that the solution is essentially identical to the RANS solution, even if Δ is much less than δ. A value larger than 8 would delay LES in even larger regions, which would be safer in the sense of avoiding Modeled Stress Depletion (MSD), but is undesirable overall. It is conceivable that models very different from S-A would make r_d approach 0 at $d = \delta$ differently enough to require a modest adjustment of f_d.

The application of the above procedures to S-A-based DES, which is used from here on, proceeds by re-defining the DES length scale $\tilde{d}$:

$$\tilde{d} \equiv d - f_d max(0, d - C_{DES}\Delta), \tag{4}$$

setting f_d to 0 yields RANS ($\tilde{d} = d$), while setting it to 1 gives DES97 ($\tilde{d} = \min(d, C_{DES}\Delta)$). For DES based on most of the possible RANS models, DDES will consist in multiplying by f_d the term that constitutes the difference between RANS and DES, as in (4).

Simulation Overview

The compressible Navier-Stokes equations are solved on unstructured grids using *Cobalt*.[10] The numerical method is a cell-centered finite volume approach applicable to arbitrary cell topologies (e.g, hexahedron, prisms, tetrahedron). The spatial operator uses the exact Riemann solver of Gottlieb and Groth,[11] least squares gradient calculations using QR factorization to provide second order accuracy in space, and TVD flux limiters to limit extremes at cell faces. A point implicit method using analytical first-order inviscid and viscous Jacobians is used for advancement of the discretized system. For time-accurate computations, a Newton sub-iteration scheme is employed, the method is second order accurate in time. The domain decomposition library ParMETIS[12] is used for parallel implementation and communication between processors is achieved using Message Passing Interface.

The computations summarized in the next section have been performed on unstructured grids comprised of 6.696×10^6 cells (non-rotating grid) and 6.380×10^6 cells (rotating grid). A cross-section in the vicinity of the non-rotating golf ball and the rotating golf ball is shown in Figure **??**. The grids were created using Gridgen**?** and are comprised of prisms near the ball surface and tetrahedra away from the wall. The spacing from the golf ball surface, on which no-slip conditions are applied, to the cell center nearest the wall is within one viscous unit (IS THIS TRUE????). Farfield conditions are applied at the outer boundaries of the computational domain that lie in the plane of the freestream velocity vector. The outer boundaries are located 14 diameters from the golf ball surface.

The Reynolds number based on golf ball diameter and freestream velocity for the results presented in the next section is 1.58×10^2. The separated flow is approximated by computing fully-turbulent solutions.

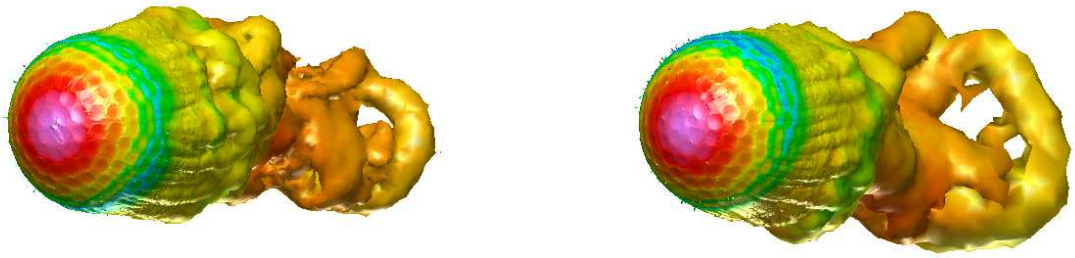

(a) (b)

Fig. 2 Isosurfaces of the instantaneous vorticity colored by pressure. (a) Non-rotating DDES; (b) Rotating DDES.

Results

Isosurfaces of the instantaneous isosurface (which are colored by pressure) at which the freestream velocity is equal to zero on the non-rotating golf ball are shown in Figure 2a for non-rotating DDES, Figure 2b for rotating DDES. The figures show that the three-dimensional structure of the wake appears qualitatively similar in the predictions obtained by each model. Owing to the strong instabilities governing the flow, the wake structure quickly develops a complex, three-dimensional character.

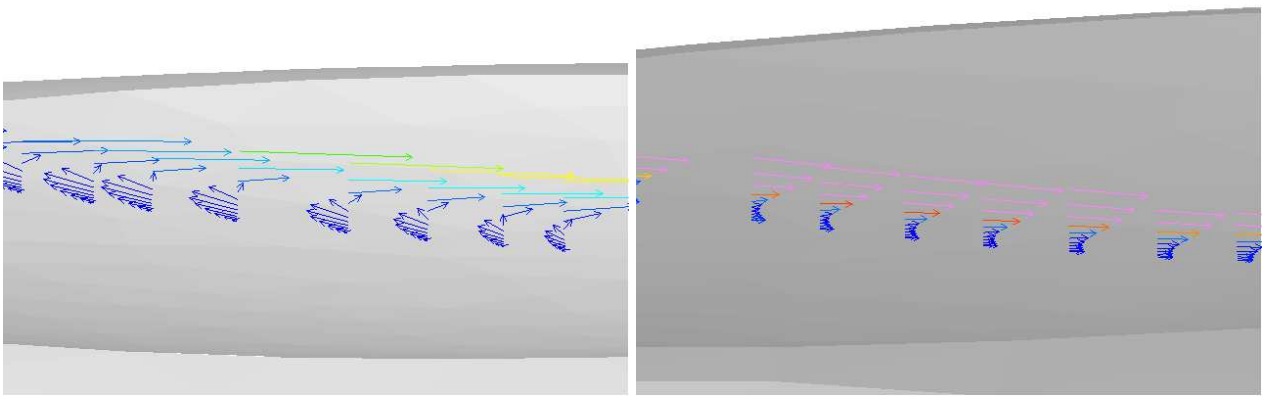

(a) (b)

Fig. 3 Velocity vectors colored by eddy viscosity (a) Non-rotating DDES; (b) Rotating DDES.

Velocity vectors colored by the eddy viscosity at a single instant are shown in Figure 3 for non-rotating DDES (in a) and rotating DDES (in b). Analogous to the behavior in Figure 2, the eddy viscosity fields for each of the models appear similar. Figure 2 and Figure 3 show that DDES does not interfere with the character of the flow structure and turbulence model in the wake.

Time histories of the drag and lift coefficients for the non-rotating model are plotted in Figure 4a and b, respectively. The black curve shown in both plots is a modified version of DDES in which the LES region is not activated until approximately $r/D = 1.025$. It is noteworthy to observe that the mean drag coefficient for the modified DDES is approximately 0.25, in good agreement with the experimental predictions of Bearman and Harvey[4] and Choi.[5] The lift force oscillations in Figure 4b display the modulation characteristic of bluff body flows and reflect the complex processes governing the wake.

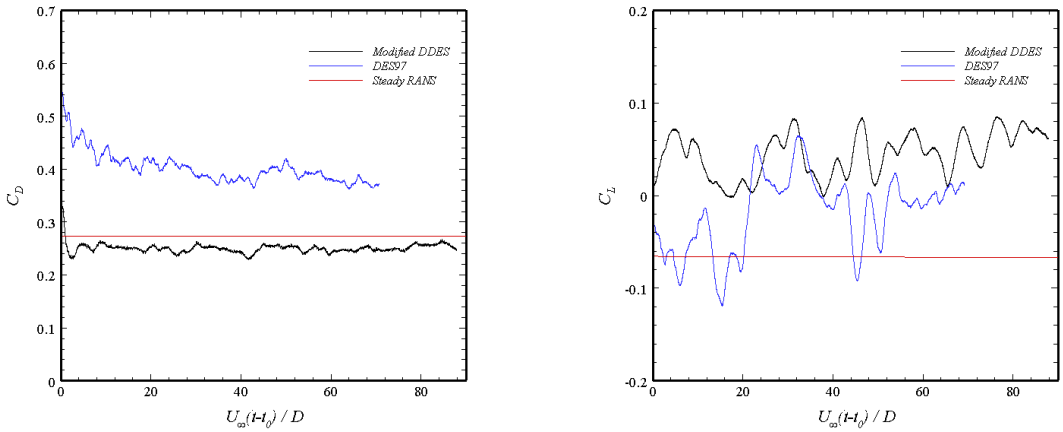

(a) (b)

Fig. 4 Time history of the drag (in a) and lift (in b) force coefficients.

Summary

Turbulence predictions at $Re = 1.58 \times 10^2$ show that there are significicant differences in the flowfield around the golf ball depending on the model used. The distinctions between the models are evident in the data for the force histories and mean drag, and the modified DDES values are in good agreement with the previous experiments performed by Choi *et al.*[5] Flow visualizations show that there the structural features resolved are very similar for the non-rotating and the rotating cases. The massively separated flow around a golf ball is a natural case for DES and the current grid does cause a change to the turbulence model which could adversely impact boundary layer prediction. Computations for a range of grid refinement and dimple patterns will be reported in the full paper, along with investigation into the influence of the Reynolds number on the solution results. These additional computations will further stress boundary layer prediction, enable a detailed view of the operational differences between the turbulence models, and also provide insight into the asymptotic values of quantities such as the drag coefficient around a golf ball in subcritical flow.

References

[1]Spalart, P. and Allmaras, S., "A One-Equation Turbulence Model for Aerodynamic Flows," *La Recherche Aerospatiale*, , No. 1, 1994, pp. 5–21.

[2]Spalart, P., Jou, W., Strelets, M., and Allmaras, S., "Comments on the Feasibility of LES for Wings, and on a Hybrid RANS/LES Approach," *First AFOSR International Conference on DNS/LES*, Ruston, Louisiana, 1997.

[3]Spalart, P. R., Deck, S., Shur, M. L., Squires, K. D., Strelets, M. K., and Travin, A., "A new version of Detached-Eddy Simulation, resistant to ambiguous grid densities," *Theo. Comp. Fluid Dynamics*.

[4]Bearman, P. W. and Harvey, J. K., "Golf Ball Aerodynamics," *Aeronautical Quarterly*, Vol. 27, No. 2, May 1976, pp. 112–122.

[5]Choi, J., Jeon, W. P., and Choi, H., "Mechanism of drag reduction by dimples on a sphere," *Physics of Fluids*, , No. 18, April 2006.

[6]Squires, K. D., "Detached-Eddy Simulation of Turbulent Flows," *von Karman Institute for Fluid Dynamics Lecture series on "Large Eddy Simulation and Related Techniques: Theory and Applications"*, Rhode-Saint-Genese, Belgium, March 2006.

[7]Forsythe, J. R., Squires, K. D., Wurtzler, K. E., and Spalart, P. R., "Detached-Eddy Simulation of Fighter Aircraft at High Alpha," *Aerospace Sciences Meeting*, AIAA, Reno, NV, 2002, pp. 1–11.

[8]Menter, F. and Kuntz, M., "Adaptation of eddy-viscosity turbulence models to unsteady separated flow behind vehicles," , pp. 339–352.

[9]Shur, M., Spalart, P., Stretlets, M., and Travin, A., "Detached-Eddy Simulation of an Airfoil at High Angle of Attack," *4th International Symposium of Engineering Turbulence Modeling and Measurements*, Corsica, May 1999.

[10]Strang, W., Tomaro, R., and Grismer, M., "The Defining Methods of Cobalt$_{60}$: a Parallel, Implicit, Unstructured Euler/Navier-Stokes Flow Solver," Aiaa paper 99–0786, Jan. 1999.

[11]Gottlieb, J. and Groth, C., "Assessment of Riemann Solvers for Unsteady One-Dimensional Inviscid Flows of Perfect Gases," *Journal of Computational Physics*, Vol. 78, 1988, pp. 437–458.

[12]Karypis, G., Schloegel, K., and Kumar, V., *ParMETIS: Parallel Graph Partioning and Sparse Matrix Ordering Library Version 1.0*, University of Minnesota, Department of Computer Science, Minneapolis, MN, 1997.